京都大学防災研究所年報 第 58 号 B 平成 27 年 6 月
Annuals of Disas. Prev. Res. Inst., Kyoto Univ., No. 58 B, 2015

Flume Experiment on Bedload Measurement with a Plate Microphone

Takahiro KOSHIBA[(1)], Tetsuya SUMI, Yasuhiro TAKEMON, and Daizo TSUTSUMI

(1) Graduate School of Engineering, Kyoto university

Synopsis

Measuring the bedload transport rate in rivers or hydraulic structures is of utmost interest to understand and quantify all sediment transport related phenomena such as sedimentation, degradation, or bed abrasion of bedrock or concrete. Two bedload measuring systems exist: the Japanese hydrophone and the Swiss geophone. Both systems are installed on the river bed and estimate transport rate based on sediment impact, but both have respective disadvantages. To improve weak points while leaving their merits, a plate microphone was developed. In this study, the calibration experiment of such plate microphone in a laboratory flume is described. In the experiments, impact data is perceived as both sound pressure and sound pulse. As a result, the nonlinear correlation between bedload transport rate and sound pressure and sound pulses are found. However, it is also clarified that fine sediments lower than 10 mm are not detectable. A detection rate is introduced showing that transport is underestimated in case of continuous sediment supply with high amount of transported sediment. Finally, it is investigated that this underestimation can be linked to the sediment bulk density and the gravel jump length.

Keywords: bedload measurement, plate microphone, sound pressure, grain size, flume experiment

1. Introduction

1.1 Background

There are more than three thousands dams in Japan for different purposes. Some of these reservoirs face severe sedimentation problems and require urgent sedimentation management. One advanced technique in Japan is the sediment bypass tunnel (SBT) to reduce suspended and bed load depositions in reservoirs by routing the incoming sediments around the dam (Sumi et al. 2004, Auel and Boes 2011). Japan and Switzerland are leading countries in SBT operation. However, measuring and quantifying the sediment movement in a SBT is challenging and a topical research subject (Hagmann et al. 2015). Especially invert abrasion is a severe problem facing most SBT which is directly connected to increasing maintenance cost (Auel and Boes 2011, Baumer and Radogna 2015, Jacobs and Hagmann, 2015, Nakajima et al. 2015).

It is essential to clarify the hydraulic characteristics and sediment transport mechanisms in a SBT. The invert abrasion is caused by a combination of high flow velocities and a high sediment transport rates (Auel and Boes 2011, Auel 2014). The sediment which is routed downstream of the dam during floods is also important regarding river environmental aspects. Various techniques have been developed to monitor suspended sediment, for example by using turbidity current meter.

However, there are limited techniques for field observation of bedload sediment transport to understand the mechanisms and to quantify transport rates.

In a study at the Hodaka Sedimentation Observatory, DPRI, Kyoto University, bedload transport rates were measured by pipe hydrophones (Tsutsumi et al. 2008). A hydrophone steel pipe detects the sediment rate by the number of pulses and sound pressure caused by gravel hits. Another technique developed in Switzerland is the geophone containing both a steel plate and vibration sensor (Rickenmann et al. 2012). Switzerland also has rivers in the mountains similar to Japan. A geophone system was installed the first time in an SBT at the Solis dam and started operation from 2013 (Hagmann et al. 2015). Both indirect monitoring techniques, the pipe hydrophone and the plate geophone, have particular weak points. For instance, the hydrophone often underestimates bedload when the pulses are successive and overlap. Also the hydrophone easily deforms when hit by large stones. In contrary, a geophone is shock-resistant but cannot detect fine sediments with a diameter smaller than 2 to 4 cm (Rickenmann et al. 2012). To improve the weak points of these two techniques with leaving their advantages, the plate microphone was developed. In this study, a new method to measure bedload transport with steel plate microphone is proposed and experimentally investigated for various hydraulic and sediment conditions. At present, research representatives from Japan and Switzerland are exchanging their studies with each other. Moreover, now the construction of Koshibu SBT is progressing and start operation in 2016. Therefore, developing an innovative monitoring technique to quantify bedload sediment transport is a topical issue.

1.2 Existing Measurement Techniques for Bedload Transport Rates

The pipe hydrophone system is already installed in some rivers in Japan (Fig. 1). It consists of a rounded metal pipe installed directly in the river bed. When gravels and sand pass over the pipe, the number of hitting particles is measured by the hydrophone microphone based on sound pressure. The plate geophone (Fig. 2) was developed and used in Switzerland, but is also used in Italy, Austria and other European countries. The geophone system consists of a 50 cm by 36 cm steel plate with a geophone sensor mounted below, embedded in a steel frame and installed directly in river bed. A geophone estimates sediment transport rates based on the plate vibration expressed in voltage caused by the passing sediment. The geophone system was already developed in the early 1990ies before the microphone was developed in Japan. Each measuring technique has the similar sediment rate measuring principle. However, both systems have different features caused by the difference of sensors and design (Table 1).

Fig. 1 Hydrophone installed on the Yodagiri river, Nagano, Japan (courtesy of T.Koshiba).

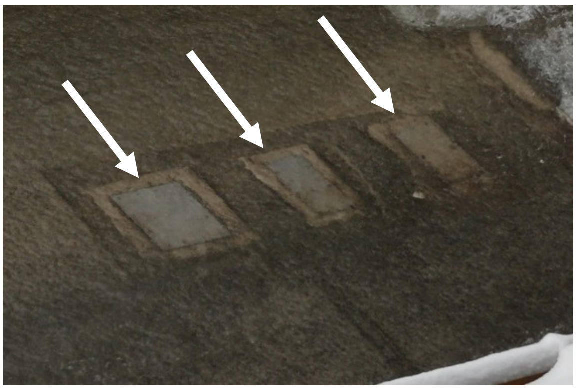

Fig. 2 Geophone installed on the Ashiarai-dani, Gifu, Japan (courtesy of T.Koshiba).

Fig. 3 Plate microphone in the test flume. Design similar to geophone system (courtesy of T.Koshiba).

Table 1 Comparison of Geophone and Hydrophone

	Hydrophone	Geophone
Made in	Japan	Switzerland
Shape	Steel pipe	Steel plate
Principle	Counting number of pulses based on sound pressure	Measuring voltage of vibration caused by overpassing sediment
Merit	● Inexpensive system setup ● Detecting small grain size of approx. 2mm	● Strong for large stones. ● Thicker plate can deal with larger stones like megalith
Demerit	● Deform easily when large stones hit ● Underestimate bedload rate during high sound or large amount of sediment	● Initial installation cost is high ● Minimum detectable grain size is approx. 10mm

1.3 Plate Microphone

By considering the demerits shown in Table 1, the plate microphone (Fig.3) was developed in Japan as a method to measure the bedload transport rate. The Microphone system consists of a steel plate like the geophone and measures bedload transport rates on the base of sound pressure like the hydrophone. Moreover, plate microphone also measures sound pressures in addition to the number of pulses. The sound pressure is expected to help measuring sediment rate accurately. With these characteristics, the plate microphone is expected to record hitting sounds of fine sediment and also to be robust against hitting by coarse sediment.

1.4 Objectives

There is a gap in research regarding the experimental investigations of plate microphones, the design and its configurations prior implementation in the field. Therefore, this study attempts to optimize the plate microphone configurations for field investigations in Koshibu SBT. One of the main objectives is to understand the functioning of the plate microphone for various sediment transport and flow conditions. The experimental study in the laboratory flume has the following objectives:

- To find a correlation between sediment transport rate and acoustic pulses of the microphone.
- To clarify the linkage between sediment transport rate and integrated sound pressure.
- To examine the minimum detectable grain size that can be measured by the plate microphone.

2. Experimental Setup and Conditions

2.1 Design of Plate Microphone Instrument

2.1.1 Laboratory Flume test

The experiments of this study were carried out in a flume facility at the VAW hydraulic laboratory of ETH Zurich, Switzerland. A schematic view of the experimental setup and parameters are shown in Fig. 4. The experimental setup consists of an elevated water supply tank that discharges the water to a rectangular flume with inner dimensions of 0.50 m width, 0.60 m height, and 8.00 m length. The plate microphone is placed just before the flume outlet at 7.56 m from the inlet. The discharge is controlled by a gate valve. The flow velocity is controlled by a jetbox, which has gate, and the flow velocity is obtained by measuring the discharge with a magnetic flow meter and the flow depth with point gauge measurements. At the flume end the water plunges into a stilling basin.

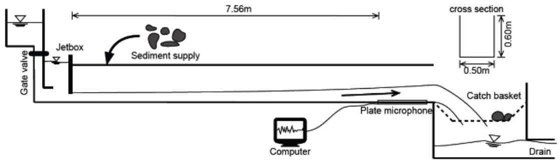

Fig. 4 Schematic view of the laboratory test flume.

2.1.2 System of Plate microphone

The dimensions of the plate microphone used in this experiment are shown in Fig. 5. The system consists of three parts: a steel plate, a microphone and a data-logger. The geometry of the steel plate are: 49.2 cm width, 35.8 cm length, and 1.5cm thickness. Water and sediment flows are perpendicular to the plate width. The microphone which detects the sound wave is installed under the plate and connected to the data-logger.

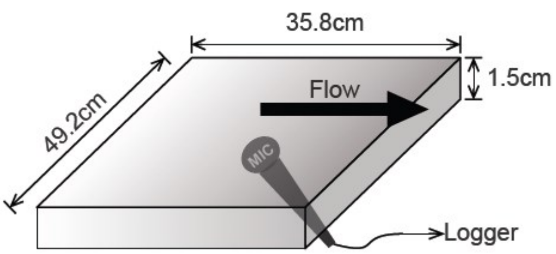

Fig. 5 Schematic view of plate microphone

2.1.3 Condition of Sediment Characteristics

In this experiment, five types of gravels are used. Grain sizes and average weight of used gravel are shown in Table 2. The specific gravity of sediment σ is 2.7 g/cm^3. The tested sediment has various shapes including rounded, irregular and angular particles. Fig. 6 gives an example of D_s = 100 mm gravel, with D_s = decisive grain diameter.

Table 2 Dimensions of tested sediment

Grain Size (D_s)	B-axis [mm]	Average Weight [g]
2 mm	2.00-2.36	3.2 of 200 particles
5 mm	5.00-6.00	14.3 of 100 particles
10 mm	10.0-12.0	2.1
50 mm	45.0-55.0	159.2
100 mm	95.0-105.0	2937.6

Fig. 6 Image of tested sediment stones of D_s = 100 mm. (courtesy of T.Koshiba)

2.1.4 Recording Systems

Several parameters were measured during each experiment, namely the (a) sound waveform, (b) pulses with 6 amplitudes, and (c) sound pressure. The mechanisms of these three parameters are as follows:

(a) Sound waveform

The sound waveform is raw data collected by the microphone. A value of voltage was recorded every 20 μs. Fig. 7 shows one example of a raw waveform output.

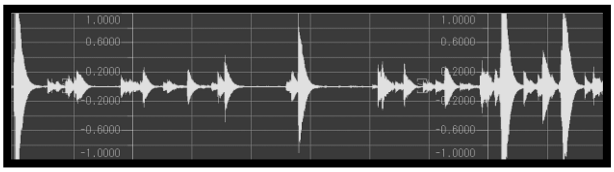

Fig. 7 Example of waveform data

(b) Pulses

The pulse is determined by processes shown in Fig. 8. First, the sound waveform is 20-times amplified by a preamplifier and transformed into an absolute value. Then, the specific frequency is extracted by a bandpass filter and an envelope curve of this wave is recorded as the waveform and amplified 10-times again (Fig. 9). The extracted wave is exported to 6 different channels, in which the wave was amplified 2, 4, 16, 64, 256, and 1024 times. The amplification was made to find the best value to detect the highest number of particle impacts. Finally, the output pulses are logged by the logger if the amplitude is larger than the threshold value of 2 V. Fig. 10 explains this process.

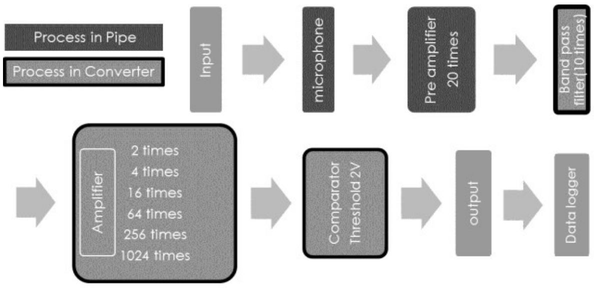

Fig. 8 Flowchart of converting wave data.

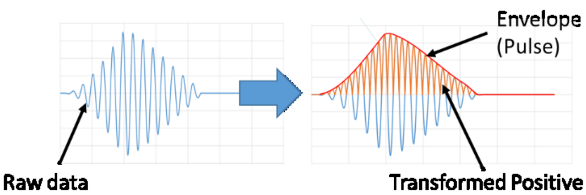

Fig. 9 Process of conversing raw waveform data.

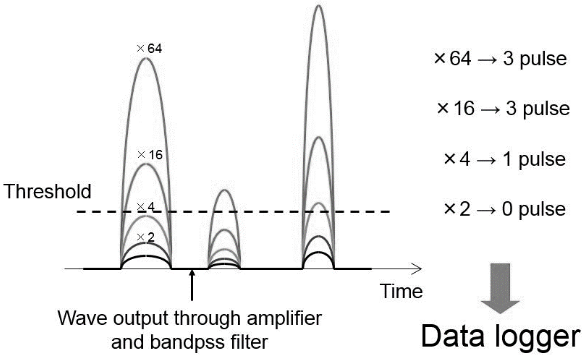

Fig. 10 The process of transferring counting pulses into pulses.

(c) Sound pressure

When sediment transport rate is high, the number of pulses becomes low or zero due to overlapping of each separated pulse. Fig. 11 shows a case where the number of pulses are underestimated. In this case, the number of pulses which are higher than the threshold is only one, nevertheless the actual pulse number is eight.

To counter this problem, the sound pressure S_p is also measured. Fig. 11 also explains the principle of calculating S_p. The sound pressure is the sum of the values which are measured with a constant sampling time by the logger divided by a constant interval dT (in

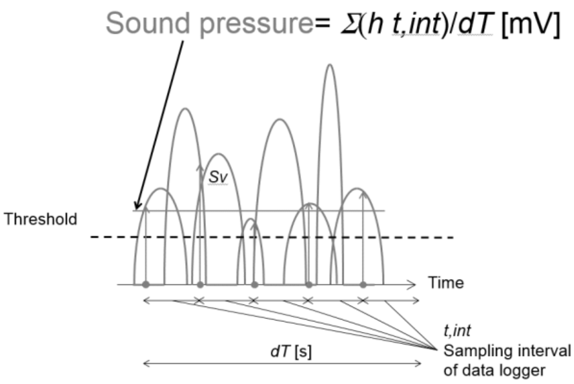

Fig. 11 The example case that the number of pulses are underestimated and the principle of recording sound pressure

this case, this interval dT is 10 seconds). Hence, S_p is the average value of the output voltage.

2.2 Experimental Procedure

The experimental procedure is identical for all tested configurations. Prior to each experiment, the sediment and plate conditions were adapted. The pump starts working, then the electromagnetic flow meter and a valve are used to setup the design discharge as a target value. Then the data-logger switched on. The flow depth was kept constant, and sediment grains are supplied manually within 5 seconds directly downstream of the jetbox. Finally, the plate microphone sensor measured the impacts and outputs were recorded in the PC.

2.3 Experimental Conditions

The experimental conditions are presented in Table 3. The flow depth was kept constant with 0.08 m, whereas the discharge Q and velocity V were varied two times, represented as *low* and *high flow* conditions. Q_s is the amount of sediment. Normally, the flow velocity in SBT is even higher and often reaches more than 10 m/s (Auel and Boes 2011).

A constant sediment weight of 50 g for both grain sizes, D_s = 2 mm and 5 mm, are supplied. For D_s = 10 mm, 50 mm, and 100 mm, a fixed number of 20 stones was added manually to the flow.

Moreover the experiments can be divided into two types: continuous-supply, and single-supply. Continuous-supply is repeated 50 times for every condition, whereas single-supply experiments are carried out one time throwing 10 stones consecutively (conducted for D_s = 2 mm, 5 mm, 10 mm, and 50 mm). For D_s = 100 mm, the experiment is repeated two times throwing only three consecutive stones. The purpose of single-supply type is to examine the output of a single particle.

Table 3 Experimental Conditions

	Flow		Sediment	
Case No.	Q [m³/s]	V [m/s]	Ds [mm]	Qs [g]
1	0.10	2.82 (Low)	2	50
2	0.10	2.82 (Low)	5	50
3	0.10	2.82 (Low)	10	50
4	0.10	2.82 (Low)	50	20stones
5	0.10	2.82 (Low)	100	20stones
6	0.18	5.08 (High)	2	50
7	0.18	5.08 (High)	5	50
8	0.18	5.08 (High)	10	50
9	0.18	5.08 (High)	50	20stones
10	0.18	5.08 (High)	100	20stones

3. Experimental Results and Discussions

3.1 Relationship between Sediment Transport Rate and Sound Pressure

Fig. 12 shows the relationship between the sediment transport rate and the sound pressure for continuous-supply experiments using low flow conditions. Only few of the D_s = 2 mm grains were detected. The figure clearly depicts that the sediment of sizes D_s = 2 mm, 5 mm and 100 mm vary widely between zero and about 100 mV of sound pressure indicating a positive correlation of increasing S_p with increasing diameter. However, the 10 mm, 50mm, and 100 mm are classified in three groups all ranging between about 60 to 200 mV impeding a clear correlation of S_p to the grain size.

Fig. 13 shows the plot of both single-supply and continuous-supply experiments of D_s = 100 mm at low flow conditions. The straight line connects the origin and single-supply uniform grainsize experiment (D_s = 100 mm, average of throwing two times three consecutive particles) assuming that the sound pressure is proportional to the supplied sediment weight. However, analyzing the continuous-supply experiments reveals that with increasing impact number, hits of different particles will overlap, which damps the sound pressure lower than the proportional relationship. The data of continuous-particles experiments appear to be lower than what is expected from the relationship assumed for the single-supply experiments. In order to confirm this theory, it's necessary to have more experiment with a wider range of sediment transport rates.

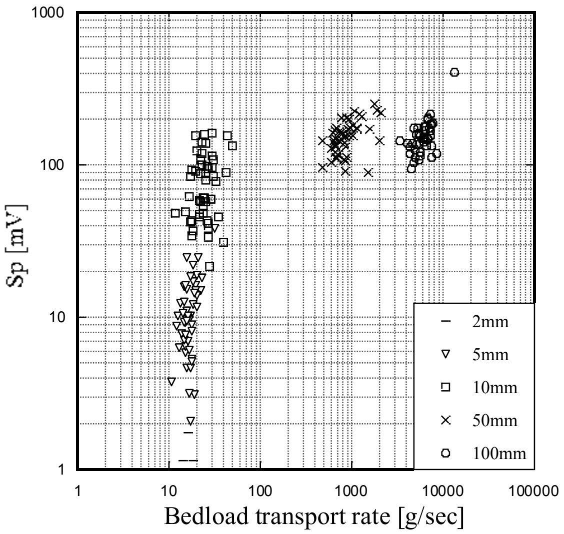

Fig. 12 Relationship between sediment transport rate and sound pressure for continuous-supply (Low flow)

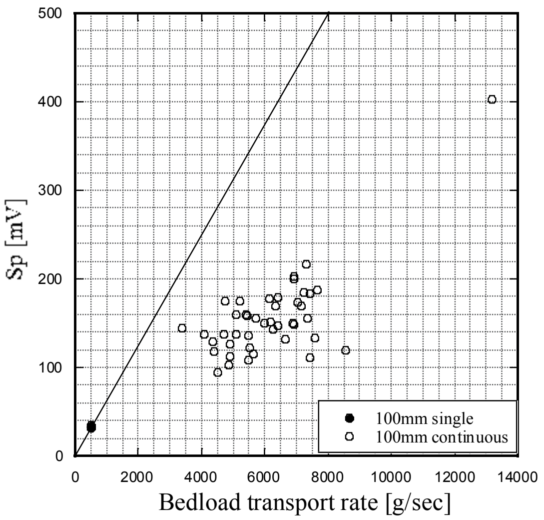

Fig. 13 Correlation between sound pressure and bedload transport of continuous-supply and single-supply (Low flow, D_s = 100 mm).

3.2 Relationship between the amplitude and the number of pulses

Fig. 14 shows the relationship between the amplitude and the number of pulses for high flow conditions of D_s = 10 mm. This graph reveals that the number of pulses increases with increasing amplitude. The reason is that more particles exceed the amplitude threshold, thus more particles are detected.

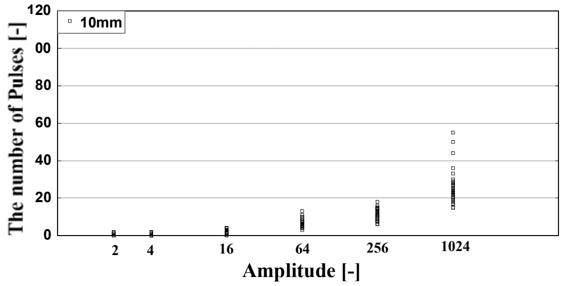

Fig. 14 Relationship between amplitude and the number of pulses in the continuous-supply (High flow, D_s = 10 mm)

3.3 Analysis of Plate Microphone Governing Parameters

3.3.1 Pulses Detection Rate

To know how much sediment is detected by the plate microphone compared to the total sediment rate, the detection rate R_d was defined. R_d is defined as the number of detected pulsed divided by total supplied number of gravels. This means that for R_d > 1.0 a particle hits the plate more than one time.

Fig. 15 and Fig. 16 show the relationship between R_d and the amplitude in order to identify the best amplitude to detect all particle impacts. Fig. 15 shows the low flow and Fig. 16 the high flow conditions, respectively.

These figures reveal that R_d of D_s = 2 mm and 5 mm are low making it hard to estimate an accurate sediment transport rate. However, the detection rate for particles with D_s > 10 mm is good in general for both low and high flow conditions, if a minimum amplitude of 16, better 64 or 256 is considered.

However, there are differences between the low flow and high flow conditions for D_s = 50 mm and 100 mm. In both cases R_d increases with amplitude, but for the low flow case R_d even exceeds 1. That can be explained by the bedload transport mode, where particles are rolling and hitting the plate more times. For the high flow experiment, R_d does not exceed 1 for amplitudes 16 to 256. It is assumed that the gravel saltates due to high flow velocity and does not hit the plate often. However, surprisingly the amplitude 1024 largely exceeds R_d = 1. The reason is that the water induced noise causes values R_d > 1 at the highest amplitude. According to both figures R_d for D_s = 10 mm is around 0.5 for amplitudes 64 and 256 which can be seen as a satisfying result to detect this particle size.

Finally, it can be concluded that the optimal amplitude is 64 or 256.

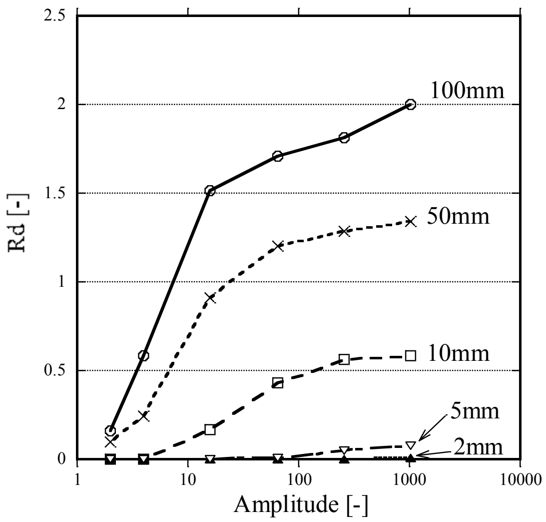

Fig. 15 Relationship between detection rate and amplitude of continuous-supply (Low flow)

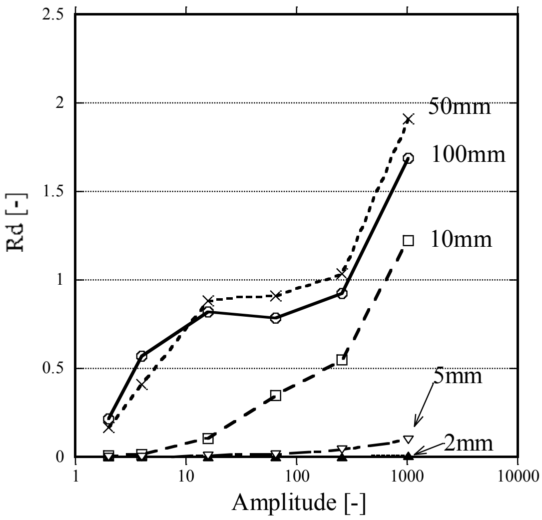

Fig. 16 Relationship between detection rate and amplitude of continuous-supply (High flow)

3.3.2 Saturation Rate

One governing parameter which influences the detection rate is the number of particles transported over the plate at the same time representing a bulk density. Hence, the saturation rate R_s is proposed as:

$$R_s = \frac{\Delta t \times P_n}{T} \quad (1)$$

Here, Δt: impact time caused by one particle hit on the plate microphone [s], P_n: the number of particle used in one experiment, T: The time between first collision of first particle to the last of the last particle in one experiment. Fig. 17 explains these parameters.

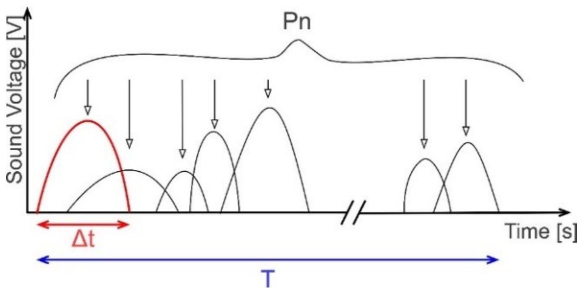

Fig. 17 Parameters which compose saturation rate

Fig. 18 shows the relationship between R_d and R_s using amplitude 64 and 256 for D_s = 10 mm, 50 mm, 100 mm, and amplitude 256 for D_s = 5 mm. According to this figure, as R_s increases R_d also tends to decrease. When R_s rises, both the waveforms which interfere each other and the sediment transported without hitting on the plate microphone increase leading to a decreased value of R_d.

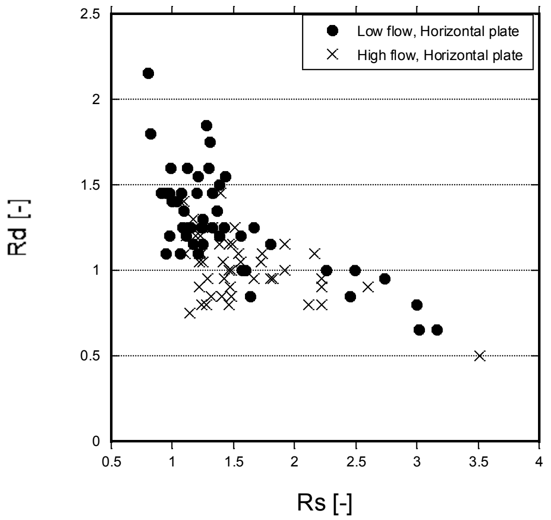

Fig. 18 Relationship between saturation rate and detection rate of continuous-supply (D_s = 50mm, Amplitude: 256)

3.3.3 Jump Length and Jump Height

It is obvious that gravel and sand jump length and height affect the relationship with R_d. Jump length and height for supercritical flows can be calculated as follows (Auel 2014):

$$\frac{H_P}{Ds} = 5.9\theta + 0.65 \quad (2)$$

$$\frac{L_p}{Ds} = 251\theta \quad (3)$$

Where, H_P: jump height, L_p: jump length. θ: Shield's parameter. θ is calculated by following formulae

$$\theta = \frac{\tau_b}{\rho G_s g Ds} \quad (4)$$

where G_s: relative density, g: gravitational acceleration and shear stress τ_b is

$$\tau_b = \rho u_*^2 \quad (5)$$

where ρ: density of water and u_*: shear velocity:

$$u_* = \sqrt{ghi_b} \quad (6)$$

With i_b = gradient of channel or energy line gradient. Since i_b of the testing flume in this experiment is 0°, i_b is represented by the energy gradient. Thus, probability based on jump height $P(H_p)$ and probability based on jump length $P(L_p)$ was calculated as follows.

$$P(L_p) = \frac{B}{L_p} \quad (7)$$

with *B* = plate length.

Calculation results of Eq. (7) are shown in Fig. 19, where R_d is given as a function of $P(L_p)$. Similar markers represent each diameter, and transparent symbols represent low flow and black one high flow conditions. Fig. 19 reveals that $P(L_p)$ increases with decreasing fluid velocity. At high flow velocities, particles tend to jump very long and hence do not hit the plate often, whereas at the low flow, particles tend to roll or only jump short distances and therefore show a higher detection rate R_d. However, particles $D_s \geq 50$ mm show satisfying $R_d \geq 1$ even for the high flow. That means that in average every particle hits the plate once although $P(L_p)$ is only about 20%. Consequently not only the jump length but also the height H_p has to be considered to calculate the hitting probability.

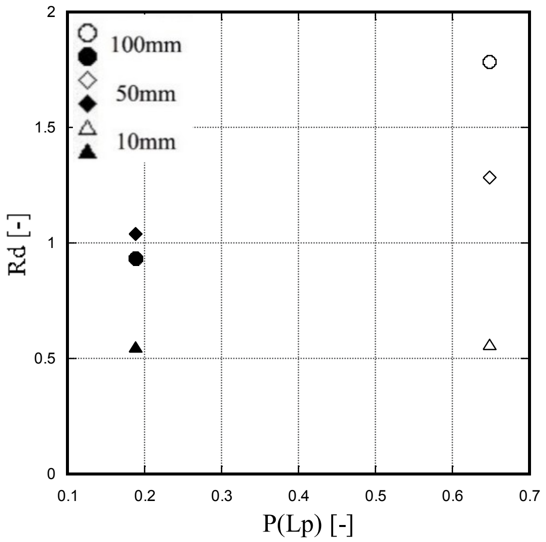

Fig. 19 The relationship between hitting probability $P(L_p)$ and detection rate of continuous-supply R_d (Amplitude: 256). Black marker: high flow, transparent marker: low flow.

3.4 New Concept of Correlation between Sound Pressure and Bedload Transport Rate

In order to estimate sediment transport rate in the river or sediment bypass tunnel, formulization of the correlation between sound pressure and bedload transport rate is necessary as shown in Fig. 14. In this section, a new concept for the formulization is proposed which should be implemented based on more experimental and field data. Fig. 20 explains this concept. In this figure, a correlation between bedload transport rate (BTR) and sound pressure is shown as curves of R_p and $P(L_p)$. The lower curve already considers the detection and saturation rate. The "Ideal S_p curve" describes the fitting curve under the condition that all sediment hit the plate microphone once. Hence, this fitting curve depends on the flow and plate conditions and varies at every river. The presented concept is useful to enlarge the estimation of sediment transport with flow conditions being beyond the experimental ones. For example, for high flows with large stones. It is necessary to clarify the ideal fitting curve and formulization of detection rate to propose an accurate measurement of bedload transport rate. An ideal fitting curve would be calculated by carrying out more flume experiments with wider varied conditions and calibration of prototype data from the river and sediment bypass tunnel.

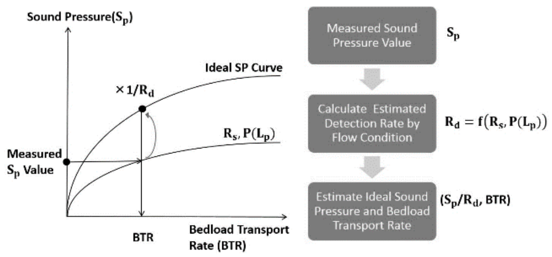

Fig. 20 Concept of correlation between sound pressure and bedload transport rate

4. Conclusion and Outlook

Innovative techniques to measure the bedload transport rate such as hydrophone and geophone are presented herein. However, it is known that both systems have particular weak points about durability and minim detectable grain size depending on instrumentation technical characteristics. The present study introduces a new instrument that combines the advances of both measuring systems namely the plate microphone. Several hydraulic, sediment, geometrical conditions have been tested in a laboratory flume and essential properties and optimized parameters of plate microphones are revealed. Moreover, a correlation between sound pressure and bedload transport rate is developed showing nonlinear behavior. It can be concluded that, the ratio of the sediment rate which passed over the plate microphone can be estimated if the detection rate is known. The optimal amplitude to detect almost all stones $D_s \geq 10$ mm is 64 times or 256 times for plate microphone. The detection rate is a significant variable affected by saturation rate and hitting probability which is based on jump length and jump height. Further investigation of various ranges of detection rates are necessary to accurately measure and estimate the bedload transport rate. It is suggested that future studies should include experiments with more varying conditions to observe the movement of particles in the water flow. The following conditions are suggested in detail: Hydraulics: Higher flow velocity of about 10 m/s to account for typical conditions in prototype SBTs. Sediment: Experiments with tracking the movement of sediment with a high speed camera.

Acknowledgements

For writing my thesis and accordingly this paper, a lot of persons helped me. Therefore, I would like to thank every of my cooperators. First, I sincerely express the greatest thanks to my supervisors Prof. Dr. Tetsuya Sumi and Assoc. Prof. Dr. Yasuhiro Takemon. Second, I thank to Dr. Daizo Tsutsumi. He helped me a lot in Hodaka sabo observatory and experiments in Zürich. Moreover, I acknowledge Assoc. Prof. Dr. Sameh Kantoush, Dr. Sohei Kobayashi, and Dr. Christian Auel. They gave me really meaningful advises and kindly checked this paper. I greatly appreciate the support of all members of VAW in ETH Zürich. They not only let us use the experimental flume but also helped so much. Finally, I deeply thank my laboratory members. Their help made me have good environment to write my thesis and this paper.

References

Auel, C. (2014): Flow characteristics, particle motion and invert abrasion in sediment bypass tunnels. Doctoral dissertation, ETH Zürich, No. 22008).

Auel, C. and Boes, R.M. (2011). Sediment bypass tunnel design – review and outlook. *Proc. ICOLD Symposium „Dams under changing challenges“* (A.J. Schleiss & R.M. Boes, eds.), 79th Annual Meeting, Lucerne. Taylor & Francis, London, UK, pp. 403-412.

Baumer, A. and Radogna, R. (2015). Rehabilitation of the Palagnedra sediment bypass tunnel (2011-2013). *Proc. Int. Workshop on Sediment Bypass Tunnels*, VAW-Mitteilung 232 (R. Boes, ed.), ETH Zurich, Switzerland, pp. 235-245.

MIZUYAMA, T., MATSUOKA, M., and NONAKA, M. (2008): Bedload measurement by acoustic energy with Hydrophone for high sediment transport rate. Journal of the Japan Society of Erosion Control Engineering, 61(1), 35-38.

Hagmann, M., Albayrak, I. and Boes, R.M. (2015).Field research: Invert material resistance and sediment transport measurements. *Proc. Int. Workshop on Sediment Bypass Tunnels*, VAW-Mitteilung 232 (R. Boes, ed.), ETH Zurich, Switzerland, pp. 123-135.

Mizuyama, T., Tomita, Y., Nonaka, M., and Fujita, M. (1996): Observation of sediment discharge rate using a hydrophone. J. Jap. Soc. of Erosion Control Eng, 49(4), 34-37.

Nakajima, H., Otsubo, Y. and Omoto, Y. (2015). Abrasion and corrective measures of a sediment bypass system at Asahi dam. *Proc. Int. Workshop on Sediment Bypass Tunnels*, VAW-Mitteilung 232 (R. Boes, ed.), ETH Zurich, Switzerland, pp. 21-32.

Rickenmann, D., Turowski, J. M., Fritschi, B., Klaiber, A., and Ludwig, A. (2012): Bedload transport measurements at the Erlenbach stream with geophones and automated basket samplers. Earth Surface Processes and Landforms, 37(9), 1000-1011.

Sumi, T., Okano, M. and Takata, Y. (2004). Reservoir sedimentation management with bypass tunnels in

Japan. *Proc. 9th International Symposium on River Sedimentation*, Yichang, China, pp. 1036–1043.

SUZUKI, T., MIZUNO, H., OSANAI, N., HIRASAWA, R., and HASEGAWA, Y. (2010): Basic study on sediment measurement with a hydrophone on the basis of sound pressure data. Journal of the Japan Society of Erosion Control Engineering, 62(5), 18-26.

TSUTSUMI, D., NONAKA, M., MIZUYAMA, T., FUJITA, M., MIYATA, S., and ICHIDA, K. (2013): Comparison of Responses from Plate Geophone and Pipe Hydrophone Sensors for Bed-load Monitoring. Disaster Prevention Research Institute annuals, Kyoto Univ., (57), pp. 385-390. (in Japanese)

TSUTSUMI, D., HIRASAWA, R., MIZUYAMA, T., SHIDA, M., and FUJITA, M. (2010): Bed Load Observation in a Mountainous Catchment by Hydrophone Equipments. Disaster Prevention Research Institute annuals, Kyoto Univ., 53(B), pp. 537-544. (in Japanese)

(Received June 11, 2015)